

Turbulence Diagnostic Simulator for Analyzing Structural Formation in Magnetically Confined Plasmas

N. KASUYA, S. NISHIMURA, M. YAGI¹⁾, K. ITOH, S.-I. ITOH¹⁾ and N. OHYABU

National Institute for Fusion Science, 322-6 Oroshi-cho, Toki, Gifu 509-5292, Japan

¹⁾ *Research Institute for Applied Mechanics, Kyushu University, 6-1 Kasuga-kouen, Kasuga, Fukuoka 816-8580, Japan*

(Received: 19 November 2009 / Accepted: 8 January 2010)

Turbulent structures affect the level of anomalous transport, and their formation mechanism is one of the crucial issues in the fusion plasmas. The structural formation mechanism in cylindrical plasmas is discussed in detail to identify the bifurcation phenomena of the turbulent structure. A three-field reduced MHD model was extended to describe the resistive drift wave turbulence, and a zonal flow and a poloidally localized turbulent structure, which has the typical temporal scale of the streamer, are formed selectively by nonlinear couplings of unstable modes. We carried out analyses to simulate the measurement with electrostatic probes, and find out the characteristic features of the turbulent states. This is the first step for integrated comparison between experiments and numerical simulations by using a long series of three-dimensional turbulence data to understand the global transport phenomena.

Keywords: turbulence simulation, diagnostic, structural formation, zonal flow, streamer, linear device, spectrum analysis

1. Introduction

The theoretical researches on plasma turbulence reveal that meso-scale structures, such as a zonal flow and a streamer, play an important role on turbulent transport [1]. Therefore, quantitative analyses of their formation and self-regulated mechanism must be carried out for understanding the global transport phenomena. Development of the experimental diagnostics can give high resolution measurements of fluctuations in space and time [2][3], and integration of several measurements will give detailed profiles of the turbulence in magnetized plasmas.

In numerical simulations, improvement of computation can produce a long series of turbulent data [4][5], and turbulence analyses can be carried out on the numerical turbulence fields [6][7]. We have been developing a turbulence diagnostic simulator, which numerically simulates plasma turbulence and data analyses on the simulation data, as same in the experiments. The simulator studies the fundamental mechanisms of turbulent structural formation, and aids the development of the data analysis technique to deepen our physical understandings.

Plasma experiments in a simple linear configuration have been revisited for quantitative understandings of the structural formation mechanism by turbulence [8]-[12]. These laboratory plasmas are suitable for carrying out detailed measurements of fluctuations, and two-dimensional measurements reveal the feature of turbulent structures [13][14] and their formation mechanisms by nonlinear mode coupling [15][16].

For the first step to study fusion plasmas, we have

author's e-mail: kasuya@nifs.ac.jp

carried out numerical simulations in cylindrical plasmas, as a minimal model for analyzing the structural formation mechanism in magnetically confined plasmas by mode coupling [6][17]-[21]. Turbulent structures, such as zonal flows and streamers have been obtained in the nonlinear saturated states, and their formation mechanisms have been studied [6]. In this paper, we analyze the time series of the physical variable from three-dimensional numerical data, and carry out correlation and spectrum analyses as carried out with electrostatic probes in experiments. The spatio-temporal profiles are obtained, which identify the bifurcation phenomena of the turbulent structure.

The paper is organized as follows. In Sec. 2, the set of model equations and parameters for the analyses are described. A zonal flow and a streamer are formed in the nonlinear simulations, and the formation mechanism is explained in Sec. 3. The correlation and spectrum analyses are carried out on the numerical turbulence fields, and characteristic features of the formed structures are discussed in Sec. 4. Then, we summarize our results in Sec. 5.

2. Drift Wave Simulation

2.1. Model

We have been developing a three-dimensional numerical simulation code of the resistive drift wave turbulence in a linear device, called 'Numerical Linear Device' (NLD, details are described in [18]). The three-field (density, potential and parallel velocity of electrons) reduced fluid model is adopted here. The plasma

has a simple cylindrical shape, and the magnetic field has only the component in the axial direction with the uniform intensity. According to experiments, high density ($n_e > 1 \times 10^{19} [\text{m}^{-3}]$) and low temperature ($T_e < 5 [\text{eV}]$) plasmas in an argon discharge are analyzed. The density of neutral particles is high even in the plasma core region [22], so the effect of neutral particles is taken into consideration. The continuity equation, the vorticity equation and Ohm's law can be used to obtain the fluctuating density, potential and parallel velocity of electrons [23]:

$$\frac{dN}{dt} = -\nabla_{\parallel} V - V \nabla_{\parallel} N + \mu_N \nabla_{\perp}^2 N + S, \quad (1)$$

$$\frac{d\nabla_{\perp}^2 \phi}{dt} = \nabla N \cdot \left(-v_{\text{in}} \nabla_{\perp} \phi - \frac{d\nabla_{\perp} \phi}{dt} \right) - v_{\text{in}} \nabla_{\perp}^2 \phi - \nabla_{\parallel} V - V \nabla_{\parallel} N + \mu_W \nabla_{\perp}^4 \phi, \quad (2)$$

$$\frac{dV}{dt} = \frac{M}{m_e} (\nabla_{\parallel} \phi - \nabla_{\parallel} N) - v_e V + \mu_V \nabla_{\perp}^2 V, \quad (3)$$

where $N = \ln(n/n_0)$, $V = v_{\parallel}/c_s$, $\phi = e\varphi/T_e$, n is the density, n_0 is the density at $r=0$, v_{\parallel} is the electron velocity parallel to the magnetic field, c_s is the ion sound velocity, φ is the electrostatic potential, T_e is the electron temperature, $d/dt = \partial/\partial t + [\phi, \]$ is the convective derivative, S is a particle source term, M/m_e is mass ratio of ion and electron, v_{in} is ion-neutral collision frequency, $v_e = v_{\text{ei}} + v_{\text{en}}$ is the sum of ion-electron and electron-neutral collision frequency, and μ_N , μ_V , μ_W are artificial viscosities. The ion cyclotron frequency Ω_{ci} and Larmor radius measured by the electron temperature ρ_s are used for the normalizations of the time and distance, respectively. The equations are solved in the cylindrical coordinate with spectral expansion in the azimuthal and axial directions assuming periodic boundary condition, where m and n are the azimuthal and axial mode number, respectively. The boundary condition in the radial direction are set to $f=0$ at $r=0$, a when $m \neq 0$, and $\partial f/\partial r = 0$ at $r=0$, $f=0$ at $r=a$ when $m=0$, where f implies $\{N, \phi, V\}$, and $r=a$ gives an outer boundary of the plasma column.

2.2. Simulation parameters

A nonlinear simulation has been performed to examine the saturation mechanism of the resistive drift wave turbulence. The relation $f(-m, -n) = \text{conj}(f(m, n))$, where f implies $\{N, \phi, V\}$, is used in the calculation to satisfy the physical quantities to be purely real in the real space. The following parameters are used: $B = 0.1 [\text{T}]$, $T_e = 2 [\text{eV}]$, $a = 10 [\text{cm}]$, length of the device $\lambda = 1.7 [\text{m}]$, $\mu_N = 1 \times 10^{-2}$, $\mu_V = \mu_W = 1 \times 10^{-4}$. Using these parameters, v_e is estimated to be $v_e = 310$ [18]. The electron collisions (v_{ei} and v_{en}) destabilize and the ion-neutral collisions (v_{in}) stabilize the resistive drift wave. Therefore, the drift wave can be excited with large v_e and small v_{in} . There is ambiguity of the value of collision frequency v_{in} , which depends on the neutral density. Therefore, v_{in} is used as a parameter for controlling the instability in our simulations. The calculation with a fixed particle source has been

carried out, where the time independent source profile is given by

$$S(r) = \frac{4S_0\mu_N}{L_N^2} \left[1 - \left(\frac{r}{L_N} \right)^2 \right] \exp \left[- \left(\frac{r}{L_N} \right)^2 \right], \quad (4)$$

with $S_0 = 5.0$, $L_N = 5 [\text{cm}]$. This source profile gives a density profile proportional to $\exp[-(r/L_N)^2]$ in a linear phase, which is flattened for $r/a = 0.2 - 0.8$ in a nonlinear phase, as described in [18]. The density profile peaked at $r=0$ destabilizes the resistive drift wave.

3. Turbulent Structural Formation

Using NLD, selective formation of the turbulent structures, zonal flow and streamer, has been studied. Linear analyses give linear growth rates and eigenfrequencies [18]. Only $n=1$ modes can be unstable with these parameters. The dispersion relation of the linear eigenmodes with $n=1$ shows weak dispersion in small m ($m < 4$), and $\partial\omega/\partial k_0 \sim 0$ with $m=4-6$.

The initial condition is given to be $f=0$ for $(m, n) = (0, 0)$ and $f = 1 \times 10^{-8} \sin(\pi r/a)$ for all the other modes, where f implies $\{N, \phi, V\}$. Simulations are performed with 256 grids in the radial direction. Fourier modes $(m, n) = (0, 0)$ and $m = \pm 1 - \pm 16$, $n = \pm 1 - \pm 16$ are taken ($m \times n = 16 \times 16$). Modes with $(m, n) = (3-6, 1)$ have the largest amplitudes in nonlinear phases, so this number of modes must be taken in calculations at least. The time evolution of each mode is calculated with Eqs. (1)–(3).

In the nonlinear saturation states, two kinds of turbulent structures have been obtained [6]; a zonal flow and a streamer. If the collision frequency is small, compared with the growth rate of unstable modes in saturated states, modulational coupling of unstable modes generates the $(0, 0)$ mode, which is the zonal flow. Figure 1 (a) shows the snapshot of the contour of the potential in the case with $v_{\text{in}} = 0.02$, where the $(0, 0)$ component is dominant. The amplitude of the $(0, 0)$ mode oscillates, and those of the other modes varies, accordingly. The limit cycle oscillation between the $(0, 0)$ mode and the perturbations contributes to the saturation [19]. Figure 1 (b) shows the time evolution of the contour of the fluctuation, where the $(0, 0)$ components are subtracted. The perturbation structure in the zonal flow case is a mixture of some modes. The dominant mode is replaced from $(4, 1)$ to $(2, 1)$, and the vortex structures are tilted and broken by the $(0, 0)$ shear flow in this duration.

If the collision frequency is large, the zonal flow remains stable, owing to strong collisional damping, and parametric coupling with modes, which have neighboring m and the frequency close to each other, forms a streamer. Figure 1 (c) shows the time evolution of the contour of fluctuation in the case with $v_{\text{in}} = 0.1$. Strong vortex is localized in the poloidal direction, and rotates to the electron diamagnetic direction. The localized structure is sustained for much longer duration than the typical time

scale of the drift wave oscillation (more than $3000 \Omega_{ci}^{-1}$). Modes with $(m, n) = (\pm 4, \pm 1)$ and $(\pm 5, \pm 1)$ are dominant in this case, and their nonlinear coupling with the mediator mode $(1, 2)$ is the origin of the sustainment of the streamer [6]. The streamer in our simulation consists of rather small number of dominant Fourier modes, $(4, 1)$ and $(5, 1)$, which are coupled with each other by means of the mediator mode $(1, 2)$, and form a quasi-mode like structure localized in the θ direction. The poloidally localized turbulent structure, which has the typical spatial and temporal scale of the streamer without the spatial scale in the radial direction, are formed by self-bunching of a couple of unstable modes in nonlinear saturation states. The nonlinear formation mechanism was quantitatively analyzed by calculating the nonlinear energy transfer to each mode [24].

The self-organized structures depend on ion-neutral collision frequency, which is the damping parameter of the zonal flow in this model. If the collision frequency is small, a zonal flow is generated, which suppresses turbulent transport. The fluctuation amplitudes are larger with smaller ν_{in} , but the turbulent fluxes have the same level, not depending on ν_{in} , because of the formation of the zonal flow [6]. On the other hand, if the collision frequency is larger than a critical value, a zonal flow is damped, and a streamer is formed. Figure 2 shows the dependencies of fluctuation energies of the potential on ν_{in} in nonlinear states. The energy components of $(0, 0)$ mode, which is the

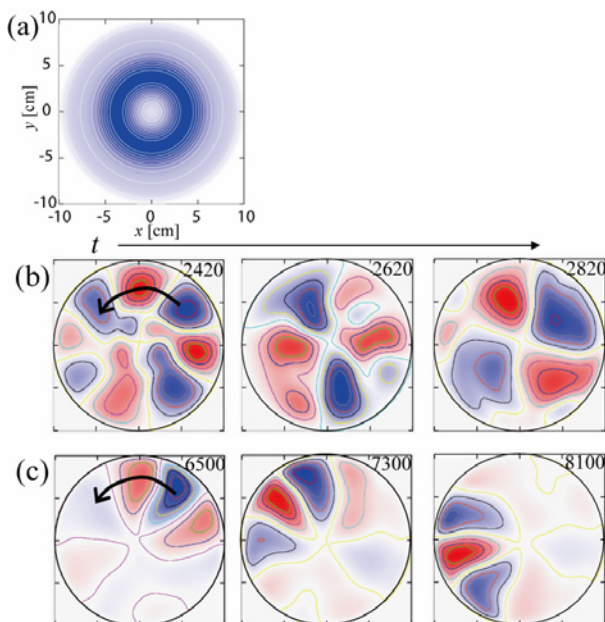


Fig. 1: Snapshots of the contour of the electrostatic potential, which is normalized by the maximum value at that time. The typical structure and the time evolution of the contour of the fluctuation in the zonal flow case with $\nu_{in} = 0.02$ are shown in (a) and (b), respectively. The time evolution of the contour of the fluctuation in the streamer case with $\nu_{in} = 0.1$ is also shown in (c).

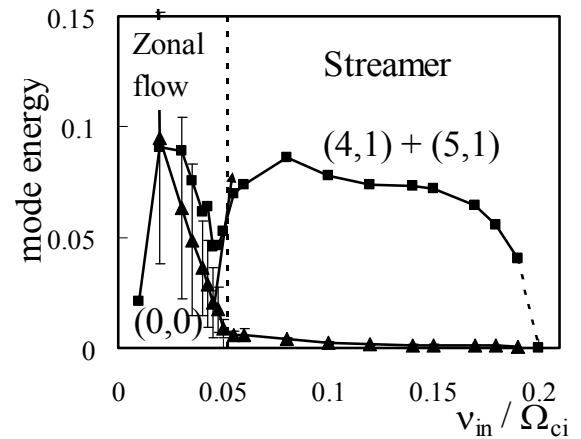


Fig. 2: Dependencies of the fluctuation energies of the electrostatic potential on ν_{in} . Energies of $(0, 0)$ mode and the sum of $(4, 1)$ and $(5, 1)$ modes, which are the zonal flow and the streamer component, respectively, are shown.

zonal flow, and the sum of $(4, 1)$ and $(5, 1)$ modes, which form the streamer, are shown. The zonal flow amplitude is small and the streamer modes are excited when $\nu_{in} > 0.052$. As ν_{in} is decreased, the zonal flow begins to be excited. There are two dominant energy exchange paths from $m \neq 0$ mode by mode coupling in this case. One is that to $(0, 0)$ mode to form the zonal flow, and the other is that to the mediator mode $((1, 2)$ in this case) to form the streamer. These two kinds of structural formation mechanisms are involved, but only one of the structures can appear in stationary states from their competitive nature. When the zonal flow is formed, the $E \times B$ shearing of the zonal flow breaks the phase locking of the modes, so the streamer is not formed, even though amplitudes of the modes are large. The streamer is selectively formed to keep the particle balance as long as the drift wave is unstable. This prediction has guided the experimental discovery of the streamer on the experimental device LMD-U [25].

4. Comparison of Spatial and Temporal Structures

In laboratory plasmas, the electrostatic probe measurement is useful to obtain fluctuation data with high spatial and temporal resolutions in experiments [25]. A transition between two turbulent states has been observed in the linear device, and the spatio-temporal spectra were measured with a multiple probe array [26]. Two kinds of turbulent structures are obtained in our simulations. We carry out analyses resemble to the single and multi probe measurements on the time series of three-dimensional fields, as described in the previous section, to clarify the difference of the turbulent structures. This is preparation of more sophisticated comparison between experiments and numerical simulations of plasma turbulence.

4.1. Temporal structure from a signal at a single point

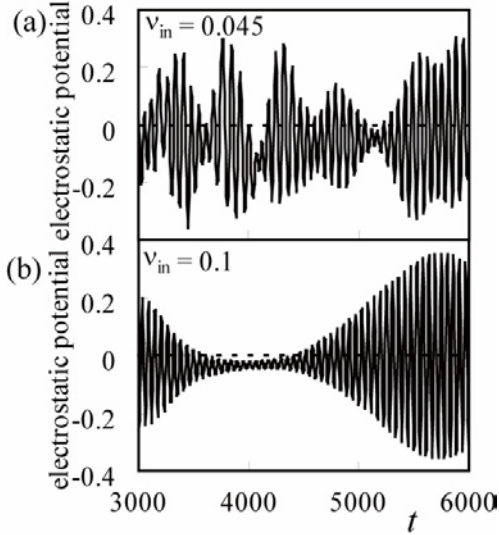


Fig. 3: Time evolutions of the potential at $r/a = 0.5$, $\theta = 0$ and $z/\lambda = 0.375$ when $v_{in} =$ (a) 0.045 (zonal flow case) and (b) 0.1 (streamer case).

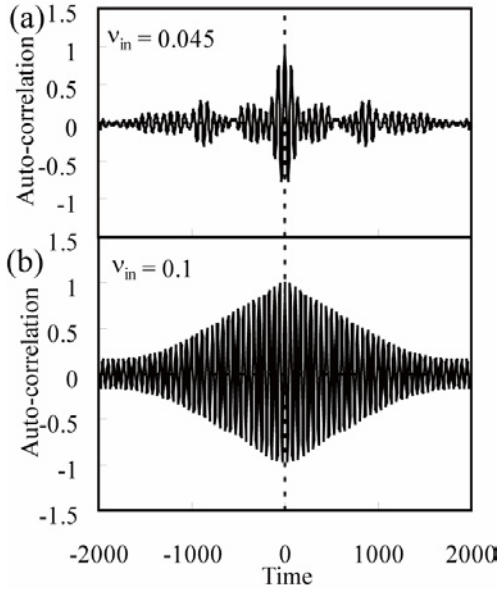


Fig. 4: Auto-correlations of the potential fluctuations at $r/a = 0.5$, $\theta = 0$ and $z/\lambda = 0.375$ when $v_{in} =$ (a) 0.045 and (b) 0.1.

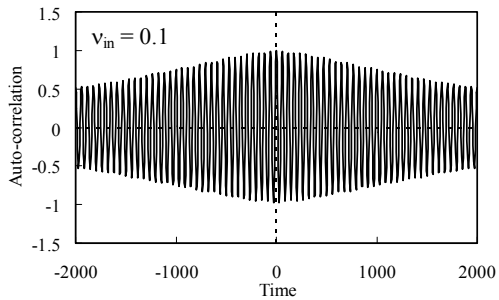


Fig. 5: Auto-correlation of the potential fluctuations, calculated on the streamer frame at $r/a = 0.5$ and $z/\lambda = 0.375$ when $v_{in} = 0.1$.

Firstly, we show the time evolution of the potential at a fixed point (Fig. 3). This corresponds to a signal from a single probe. The fine scale oscillation and its envelope correspond to the drift wave oscillation and the turbulent structure, respectively. The cases with $v_{in} = 0.045$ and 0.1 are shown as typical examples of the zonal flow and streamer, respectively. In the zonal flow case, the magnitude of the envelope abruptly changes in a few times of the drift wave oscillation period. On the other hand, the time evolution is rather periodic in the streamer case. The period of the envelope variation is about 70 times of the drift wave oscillation period, corresponding to the rotation period of the poloidally localized structure. When the streamer comes to the observation point, the amplitude becomes larger. To describe the difference of the temporal variations, the auto-correlation of the signal is calculated (Fig. 4). The correlation time is much larger in the case of the streamer than that of the zonal flow.

In the rotating frame with the velocity of the streamer propagation, the streamer stands the same poloidal position, and the life time of the streamer can be estimated. Figure 5 shows the auto-correlations of the potential fluctuation on the streamer frame when $v_{in} = 0.1$ by calculating the auto-correlation in the position where the envelope of the fluctuation has the maximum amplitude. Parameter scan showed that the life time of the streamer is longer in the less unstable case with larger v_{in} [24].

4.2. Radial correlation from signals at two points

Next, we show the correlation between two radial points to clarify the difference of the radial structure between the zonal flow and streamer case. This corresponds to the analysis using two probe signals at different radii. Figures 6 (a) and (b) show the temporal

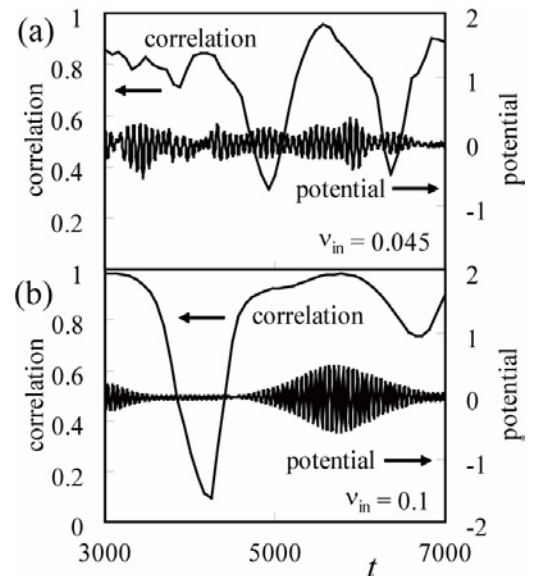


Fig. 6: Time evolutions of the radial correlation of the potential fluctuations between $r/a = 0.5$ and 0.75 at $\theta = 0$, $z/\lambda = 0.375$, when $v_{in} =$ (a) 0.045 and (b) 0.1.

evolutions of the radial correlation of potential fluctuations between $r/a = 0.5$ and 0.75 at $\theta = 0$, $z/\lambda = 0.375$ in the case of the zonal flow and the streamer, respectively. In the streamer case, the radial correlation becomes close to 1, when the streamer comes to the observation point, $t \sim 5700$. On the other hand, in the zonal flow case, the radial correlation is smaller than that in the streamer case. There is a duration when the correlation becomes close to 1 even in the zonal flow case. The streamer like structure appears intermittently, but is sustained only for a short duration, so temporally averaged correlation is smaller than that in the streamer case. The dependency of the radial correlation on v_{in} showed that the radial correlation becomes larger as v_{in} increases, and close to 1 when the streamer is sustained steadily [24].

4.3. Spatio-temporal structure from multiple signals

Finally, we show the spatio-temporal structures from the poloidal profile. This corresponds to the analysis using a poloidal probe array. The poloidal probe array is installed to clarify the structural formation in the laboratory plasmas [25]. Figure 7 shows a time evolution of the θ profile of the electrostatic potential in the case with $v_{in} = 0.1$. The localized vortex is formed (red region in Fig. 7), and its poloidal position slowly rotates to the electron diamagnetic direction. Mode matching by nonlinear coupling sustains the localized structure for much longer duration than the drift wave oscillation period.

Two-dimensional Fourier decomposition gives the spatio-temporal spectrum of the potential (Fig. 8). In the zonal flow case, low m modes with weak dispersion, which are linearly unstable, are excited and show the broad band spectrum. On the other hand, frequencies of the dominant modes are close to each other, and their harmonics are excited in the streamer case. The rather coherent spectrum appears in this case. The spatio-temporal spectra show clear difference between the zonal flow and streamer case.

The spatio-temporal spectrum shows the dispersion relation of the excited modes. The instantaneous linear dispersion relation is calculated with the density and potential profile in the nonlinear saturated state, and is compared with that of the excited modes in the streamer case (Fig. 8 (c)). The modes with $m = 3 - 5$, which have the largest amplitudes, are linearly unstable. A theoretical study showed that unstable modes with dispersion relation $\omega'(k)$ strongly induce modes with relation $\omega(k) = N\omega'(k/N)$ ($N=2,3,4,\dots$) by nonlinear coupling [27]. The sharp peaks satisfy those relations, which are plotted by dashed curves in Fig. 8 (c). In this way, diagnostics on numerical data is useful to capture the fundamental characteristics of turbulence.

5. Summary

We have carried out the nonlinear simulation of the

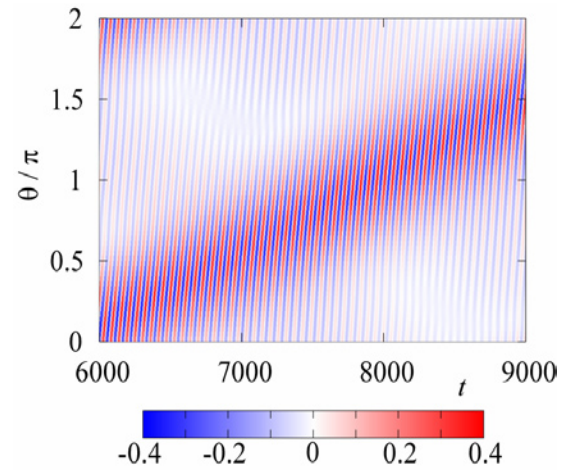


Fig. 7: Time evolution of the θ profile of the potential at $r/a = 0.5$ and $z/\lambda = 0.375$, when $v_{in} = 0.1$.

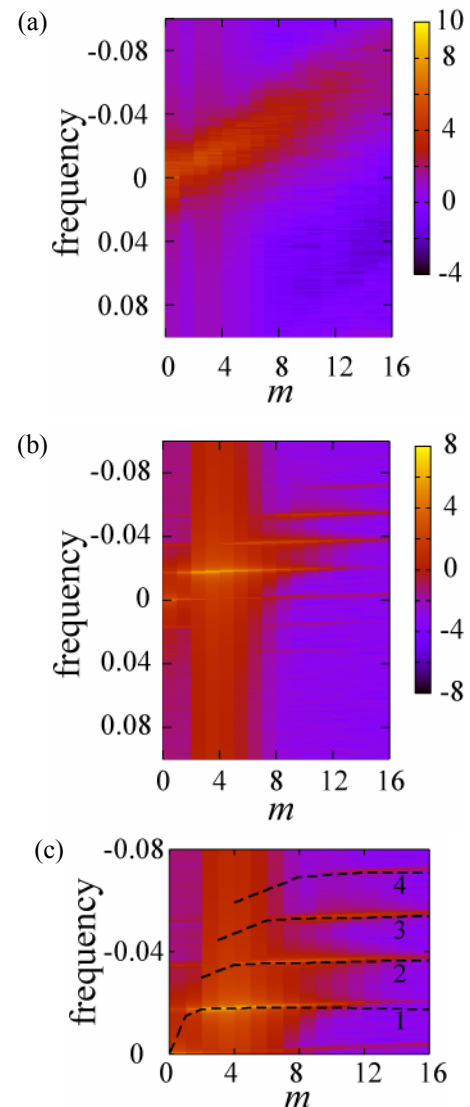


Fig. 8: Spatio-temporal spectra at $r/a = 0.5$ and $z/\lambda = 0.375$, when $v_{in} =$ (a) 0.02 and (b) 0.1. (c) Magnification of (b) with the dispersion relations of linear eigenmodes and quasi-modes induced by eigenmodes, which are indicated by dashed lines 1 and 2-4, respectively.

resistive drift wave in cylindrical plasmas. Turbulence with a zonal flow and a streamer was obtained in the nonlinear steady states. Analyses simulating the single and multi probe measurements have been carried out to clarify the difference of the spatio-temporal structures in the bifurcation. Intermittent behavior appears in the zonal flow case. On the other hand, there is long sustainment of the bunched structure with a strong radial correlation in the streamer case. A broad band and coherent spectrum appear in the zonal flow and streamer case, respectively. The frequencies of the nonlinearly excited modes agree with the theory of induced quasi-modes. We showed the analyses to clarify the difference of the turbulence structures, which is observed in our numerical simulation, in this paper. Calculations to simulate each experimental condition and detailed comparison with experiments will be future tasks.

High-order correlation analyses make quantitative estimation possible to find out which nonlinear couplings are main contributors of the structural formation, and to identify the direction of the energy transfer [28][29]. These techniques will also be applied on the simulation data.

Applying the results obtained in the simulations in cylindrical plasmas, we are developing the turbulence diagnostic simulator in toroidal plasmas. The spatio-temporal data of turbulent fields are generated by global simulation, using a fluid model describing drift-interchange instability. The analyses as same in the experiments are made on the simulation data, and comparison with experiments will be carried out.

Acknowledgement

Authors acknowledge discussions with Prof. A. Fukuyama, Prof. Y. Kawai, Prof. A. Fujisawa, Dr. S. Shinohara, Dr. Y. Nagashima, Dr. T. Yamada, Dr. S. Inagaki, Prof. P. H. Diamond, and Prof. G. R. Tynan. This work is supported by the Grant-in-Aid for Specially-Promoted Research (16002005), for Young Scientists (20760581) and for Scientific Research (19360418, 21224014) of JSPS, by the collaboration program of NIFS (NIFS09KNXN170, NIFS09KTAD009) and of RIAM of Kyushu University.

References

- [1] See reviews, e.g. P. H. Diamond, S.-I. Itoh, K. Itoh and T. S. Hahm, *Plasma Phys. Control. Fusion* **47**, R35 (2005).
- [2] A. Fujisawa, *Nucl. Fusion* **49**, 013001 (2009).
- [3] G. R. Tynan, A. Fujisawa and G. McKee, *Plasma Phys. Control. Fusion* **51**, 113001 (2009).
- [4] Y. N. Dnestrovskij, *Nucl. Fusion* **49**, 104003 (2009).
- [5] M. Yagi, S.-I. Itoh, K. Itoh and P. H. Diamond, *Contrib. Plasma Phys.* **48**, 13 (2008).
- [6] N. Kasuya, M. Yagi, S.-I. Itoh and K. Itoh, *Phys. Plasmas* **15**, 052302 (2008).
- [7] L. Lin, M. Porkolab, E. M. Edlund, J. C. Rost, C. L. Fiore, M. Greenwald, Y. Lin, D. R. Mikkelsen, N. Tsujii and S. J. Wukitch, *Phys. Plasmas* **16**, 012502 (2009).
- [8] Y. Saitou, A. Yonesu, S. Shinohara, M. V. Ignatenko, N. Kasuya, M. Kawaguchi, K. Terasaka, T. Nishijima, Y. Nagashima, Y. Kawai, M. Yagi, S.-I. Itoh, M. Azumi, and K. Itoh, *Phys. Plasmas* **14**, 072301 (2007).
- [9] G. R. Tynan, C. Holland, J. H. Yu, A. James, D. Nishijima, M. Shimada, and N. Taheri, *Plasma Phys. Control. Fusion* **48**, S51 (2006).
- [10] F. Brochard, G. Bonhomme, E. Gravier, S. Oldenb urger and M. Philipp, *Phys. Plasmas* **13**, 052509 (2006).
- [11] C. Schr oder, O. Grulke, T. Klinger and V. Naulin, *Phys. Plasmas* **12**, 042103 (2005).
- [12] V. Sokolov and A. K. Sen, *Phys. Rev. Lett.* **92**, 165002 (2004).
- [13] G. Y. Antar, J. H. Yu and G. Tynan, *Phys. Plasmas* **14**, 022301 (2007).
- [14] T. Windisch, O. Grulke and T. Klinger, *Phys. Plasmas* **13**, 122303 (2006).
- [15] K. Terasaka, S. Shinohara, Y. Nagashima, T. Yamada, M. Kawaguchi, T. Maruta, S. Inagaki, Y. Kawai, N. Kasuya, M. Yagi, A. Fujisawa, K. Itoh and S.-I. Itoh, *Plasma Fusion Res.: Rapid Comm.* **2**, 031 (2007).
- [16] F. Brochard, T. Windisch, O. Grulke and T. Klinger, *Phys. Plasmas* **13**, 122305 (2006).
- [17] N. Kasuya, M. Yagi, and K. Itoh, *J. Plasma Phys.* **72**, 957 (2006).
- [18] N. Kasuya, M. Yagi, M. Azumi, K. Itoh, and S.-I. Itoh, *J. Phys. Soc. Jpn.* **76**, 044501 (2007).
- [19] N. Kasuya, M. Yagi, K. Itoh and S.-I. Itoh *J. Phys.: Conference Series* **123**, 012026 (2008).
- [20] V. Naulin, T. Windisch and O. Grulke, *Phys. Plasmas* **15**, 012307 (2008).
- [21] G. N. Kervalishvili, R. Kleiber, R. Schneider, B. D. Scott, O. Grulke and T. Windisch, *Contrib. Plasma Phys.* **46**, 739 (2006).
- [22] M. Ignatenko, M. Azumi, M. Yagi, S. Shinohara, S.-I. Itoh and K. Itoh, *Jpn. J. Appl. Phys.* **46**, 1680 (2007).
- [23] C. Schr oder, *Experimental investigation on drift waves in linear magnetized plasmas*, Ph.D. thesis, Ernst-Moritz-Arndt-Univ. Greifswald (2003).
- [24] N. Kasuya, M. Yagi, K. Itoh and S.-I. Itoh, *Nucl. Fusion* **50**, 054003 (2010).
- [25] T. Yamada, S.-I. Itoh, T. Maruta, N. Kasuya, Y. Nagashima, S. Shinohara, K. Terasaka, M. Yagi, S. Inagaki, Y. Kawai, A. Fujisawa and K. Itoh, *Nature Phys.* **4**, 721 (2008).
- [26] H. Arakawa, K. Kamataki, S. Inagaki, T. Maruta, Y. Nagashima, T. Yamada, S. Shinohara, K. Terasaka, S. Sugita, M. Yagi, N. Kasuya, A. Fujisawa, S.-I. Itoh and K. Itoh, *Plasma Phys. Control. Fusion* **51**, 085001 (2009).
- [27] S.-I. Itoh and K. Itoh, *J. Phys. Soc. Jpn* **78**, 124502 (2009).
- [28] Y. Kim and E. Powers, *IEEE Trans. Plasma Sci.* **PS-7**, 120 (1979).
- [29] Y. Nagashima, K. Hoshino, A. Ejiri, K. Shinohara, Y. Takase, K. Tsuzuki, K. Uehara, H. Kawashima, H. Ogawa, T. Ido, Y. Kusama and Y. Miura, *Phys. Rev. Lett.* **95**, 095002 (2005).